INSTITUTE OF PHYSICS PUBLISHING JOURNAL OF PHYSICS D: APPLIED PHYSICS
J. Phys. D: Appl. Phys. **36** (2003) 1669–1674 PII: S0022-3727(03)55866-1

Three-ring filters increase the effective NA up to 1.46 in optical sectioning fluorescence microscopy

M Martínez-Corral[1], C Ibáñez-López[1], M T Caballero[2], L Muñoz-Escrivá[1] and G Saavedra[1]

[1] Departamento de Óptica, Universidad de Valencia, 46100 Burjassot, Spain
[2] Departamento de Óptica, Universidad de Alicante, PO Box 99, 03080 Alicante, Spain

Received 11 October 2002
Published 1 July 2003
Online at stacks.iop.org/JPhysD/36/1669

Abstract
Single-photon fluorescence confocal microscopy techniques can be combined with the use of specific binary filters in order to increase their optical sectioning capability. We present a novel class of axially super-resolving binary pupil filters specially designed to reach this aim. These filters let us to obtain a relevant compression of the z-response together with the reduction of the photo-bleaching effect typically inherent to apodization techniques. The fact of joining both the three-ring filters we propose in the illumination path, and the confocal detection gives rise to an important effective increase of lenses of effective numerical aperture.

1. Introduction

The improvement of the performance of optical microscopes has aimed many researches along the last decades. Conventional wide-field microscopes are close to reach their maximum efficiency through the use of the available objectives with numerical apertures (NA) up to 1.4. However, when using this kind of microscopes to image three-dimensional specimens, there is an important drawback: an image focused at a certain depth in a specimen contains blurred information from the entire one. To overcome this trouble, the use of confocal methods was proposed [1]. Confocal scanning microscopes (CSMs) are imaging systems in which the monochromatic light proceeding from a point source is focused onto a point of a three-dimensional specimen by a high-NA objective. Afterwards, the light emitted/reflected by the sample is collected by the same objective, passes through a pinhole located at the centre of the conjugate plane, and finally it is detected. The three-dimensional image is reconstructed with a computer from the intensity values acquired by three-dimensional scanning of the sample. In this symmetrical configuration both the illumination and the collection arms play the same role in the imaging properties. The main feature of confocal microscopes is their uncommon depth discrimination capacity. This capacity results from the ability of CSMs to reject the light proceeding from parts of the object that are not in focus.

However, as it is well known, due to diffraction the axial resolution of confocal set-up is, depending on the NA of the lenses, around three times poorer than its lateral counterpart [2]. This difference between axial and lateral resolution leads to an anisotropic three-dimensional-imaging quality.

Several attempts have been made to reduce the axial extent of the point spread function (PSF) of CSMs, and therefore to reduce the anisotropy of the image. We can cite the so-called confocal theta microscope [3]. In this architecture, which is only useful for fluorescence microscopy, the illumination and detection axes are tilted an angle $\pi/2$, yielding an almost isotropic PSF. Unfortunately, this technique cannot be applied in practice with systems that require the resolution provided by a high-NA objective [4].

A very ingenious, and efficient, technique to reduce the axial extent of the PSF is to create a standing-wave by the interference of two opposing wave-fronts, like in the so-called standing-wave microscopy [5] and in 4Pi-confocal microscopy [6]. Standing-wave microscopy is a nonconfocal imaging technique, so that it does not provide any improvement in the depth discrimination capacity. In contrast, in a 4Pi-confocal microscope two opposing high-NA objectives are used to coherently illuminate and detect the same point of the fluorescence specimen. In case of single-photon fluorescence the resulting PSF has a main peak that is around four times narrower than its lateral counterpart, but that goes with highly enlarged axial sidelobes. Due to these sidelobes the

single-photon 4Pi technique does not provide useful images. Nevertheless, by the use of two-photon excitation the sidelobes are removed and therefore the technique provides high quality three-dimensional images [7, 8].

An alternative technique to reduce the PSF anisotropy is based on the use of pupil filters. The drawback of using such filters in conventional imaging is that the narrowness of the PSF main peak is obtained at the expense of higher sidelobes. However, in confocal architectures this collateral effect is overcome. Along the past few years the use of purely absorbing or complex-transmittance pupil filter has been proposed to improve the resolution of confocal microscopes [9–15]. The filters these papers deal with are inserted in the illumination path, producing then an illumination PSF that is super-resolving but with high sidelobes. Due to confocality the sidelobes are strongly reduced in the confocal PSF. Therefore, the implementation of these filters is very useful in bright-field confocal microscopy. However, the filters are less useful in single-photon fluorescence confocal microscopy since the high illumination sidelobes can produce severe photo-bleaching of the specimen at the position of the strong secondary lobes. This does not happen with two-photon fluorescence microscopy. In this case the sidelobes of the illumination PSF are strongly reduced because of the square dependence of the excitation on the illumination intensity, and therefore an effective improvement of resolution is achieved with the using pupil filters [16].

In this paper we design a new set of annular binary filters composed by three transparent rings. These new filters have the ability to compress the central lobe of the axial PSF, but attenuating the increase of the axial sidelobes. Thus, we will show that by locating one of these filters in the illumination path of a single-photon fluorescence confocal microscope an important improvement of the optical sectioning capacity is achieved while the photo-damaging is reduced. In other words, we numerically show that the use of three-ring (3R) filters indeed increase the effective NA of the lenses up to 1.46.

2. Basic theory

Let us start considering the intensity PSF of a single-photon fluorescence confocal microscope, namely

$$I_{\mathrm{conf}}(z,r,\varphi) = I_{\mathrm{ill}}(r,z,\varphi)I_{\mathrm{det}}(r,z,\varphi) = |\boldsymbol{E}_{\mathrm{ill}}(r,z,\varphi)|^2\langle|\boldsymbol{E}_{\mathrm{det}}(\varepsilon r,\varepsilon z)|^2\rangle. \quad (1)$$

In equation (1) a linearly polarized illumination beam, and random polarization for the fluorescent light is assumed. Parameter $\varepsilon = \lambda_{\mathrm{exc}}/\lambda_{\mathrm{det}}$ represents the ratio between the excitation and the fluorescence wavelengths. Function $\boldsymbol{E}(r,z,\varphi)$ denotes the electric field in the focal region of an aberration-free lens illuminated by a linearly polarized wavefront. According to Richards and Wolf [17],

$$\boldsymbol{E}_\ell(r,z,\varphi) = \lfloor I_{0,\ell}(r,z) + I_{2,\ell}(r,z)\cos\varphi\rfloor\,\boldsymbol{i} + I_{2,\ell}(r,z) \times \sin(2\varphi)\boldsymbol{j} - 2iI_{1,\ell}(r,z)\cos\varphi\,\boldsymbol{k}, \qquad \ell = \mathrm{ill},\ \mathrm{det}, \quad (2)$$

where $I_{0,1,2}$ are integrals over the aperture angle θ, and φ stands for the angle between the direction of polarization of the incident field and the observation meridian plane.

To analyse the axial behaviour of a confocal microscope we centre first our attention in the axial component of the three-dimensional PSF, which is governed by the function

$$\boldsymbol{E}_\ell(r=0,z) = I_{0,\ell}(r=0,z) = \int_0^\alpha A_\ell(\theta)(1+\cos\theta) \times \exp\left(\mathrm{i}2\pi n\frac{\cos\theta}{\lambda}z\right)\sin\theta\,\mathrm{d}\theta. \quad (3)$$

In this equation, which does not depend on the polarization angle φ, n is the refractive index of the medium, α is the semi-aperture angle of the objective, and $A_\ell(\theta)$ represents the apodization function, i.e. the amplitude transmittance at the objective aperture stop. By performing the following nonlinear mapping

$$\xi = \frac{\cos\theta-\cos\alpha}{1-\cos\alpha} - 0.5, \qquad Q_\ell(\xi) = (1+\cos\theta)A_\ell(\theta), \quad (4)$$

equation (3) can be rewritten as

$$E_\ell(r=0,z_{\mathrm{N}}) = (1-\cos\alpha)\exp\left(\mathrm{i}\pi\frac{1+\cos\alpha}{1-\cos\alpha}z_{\mathrm{N}}\right) \times \int_{-0.5}^{0.5} Q_\ell(\xi)\exp(\mathrm{i}2\pi\xi z_{\mathrm{N}})\,\mathrm{d}\xi, \quad (5)$$

where we have expressed the axial position in the focal volume in terms of the normalized nondimensional variable

$$z_{\mathrm{N}} = \frac{n}{\lambda}(1-\cos\alpha)z. \quad (6)$$

Equation (6) shows that the axial PSF is governed by the one-dimensional Fourier transform of a nonlinearly mapped version, $Q_\ell(\xi)$, of the pupil amplitude transmittance. Then, the procedure to design pupil filters to tailor the axial behaviour of a confocal microscope will be simply supported on the properties of one-dimensional Fourier transformation.

3. The binary filters

Based on the properties of Fourier transformation, we designed binary filters in the past that consisted of an outer transparent ring and a central transparent circular aperture (the so-called DR filters). These filters have the ability of narrowing the central lobe of the axial PSF but at the expense of producing higher sidelobes. This family of filters became very useful in bright-field confocal microscopy [18, 19], in two-photon confocal microscopy [16] and also in two-photon 4Pi-confocal microscopy [20]. Nevertheless, these filters are not useful in practice in single-photon confocal microscopy since if they are inserted in the illumination path (to avoid light losses in the collection process), they give rise to very high axial sidelobes which can produce a severe photo-bleaching of the specimen.

To avoid this drawback we have adapted Boyer's concept [21] to the optical axis, and have designed a new type of annular binary filters. In this new design we simply add a new transparent ring centred at a radius $r = r_{\max}/\sqrt{2}$. Expressed in terms of the mapped function $Q_\ell(\xi)$ we have added a rectangle centred at $\xi = 0$. Note that these filters reproduce in a certain way the Young experiment but along the optical axis. In terms of this experiment it is easy to explain the axial behaviour of the filters. The inner and the outer rings produce an axial pattern

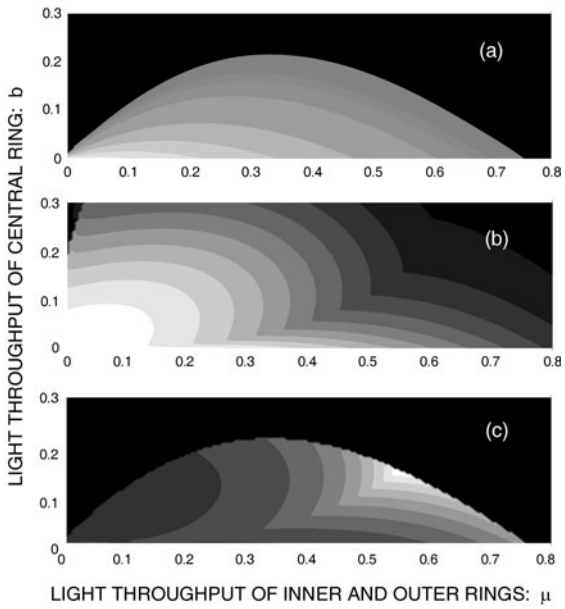

Figure 1. Merit functions to design the optimum 3R filter: (*a*) lines of constant G_A for varying values of μ and b; (*b*) lines of constant γ; (*c*) merit function G_A/γ.

in which the central lobe is narrowed but the sidelobes are high (like in a Young experiment where the slits have finite width). The central ring mainly contributes to the height of the central lobe. The combination of both effects results in an axial pattern with a narrow main peak and low sidelobes.

To select among the family of 3R binary filters the optimum one to be applied in one-photon confocal microscopy, we defined the following parameters. The axial gain, G_A, as the ratio between the full width at the half maximum (FWHM) of the axial PSF of the circular aperture and the one of the 3R filters. The ratio, γ, between the highest-sidelobe height and the main-peak height. The light throughput, μ, of inner and outer rings; and the one, b, of the central ring. The merit function for the filter-design procedure will be the ratio between the axial gain, G_A, and the relative height of the highest sidelobe, γ.

Following a procedure equivalent to the one reported in [19], it can be easily shown that the axial gain is given by

$$G_A = \left(\frac{1-\mu^3+b^3}{1-\mu+b}\right)^{1/2}. \qquad (7)$$

Thus, in figure 1(*a*) we have represented in a contour plot the lines of constant G_A for varying values of μ and b, in figure 1(*b*) we depicted the lines of constant γ, and in figure 1(*c*) the selected merit function G_A/γ. From figure 1(*c*) we find that the maximum value for this merit function corresponds to the filter with $\mu = 0.55$ and $b = 0.15$. This filter, shown in figure 2, has an axial gain $G_A = 1.14$, and a sidelobes ratio $\gamma = 0.18$. The normalized radii for the annular rings are $r_1 = 0.603$, $r_2 = 0.730$, $r_3 = 0.827$, $r_4 = 0.902$ and $r_5 = 1$.

To examine the axially super-resolving properties of the selected 3R filter we prepared a focusing experiment. The optical system was designed only to demonstrate the validity of the concept, and for practical convenience it has a low

Figure 2. Two-dimensional representation of the optimum 3R filter.

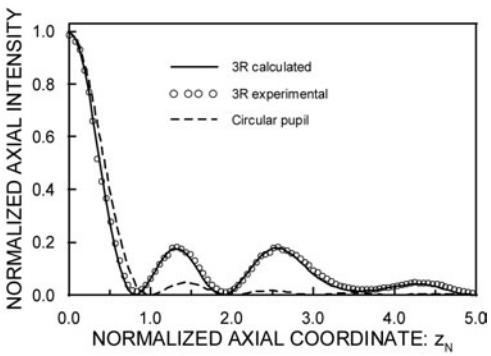

Figure 3. Normalized axial intensity distribution produced by the 3R filter, found in the calculation (——) and in the measurement (○). The dashed curve represents the axial intensity provided by a circular aperture.

NA = 0.012. In the experiment a collimated beam of $\lambda = 632.8$ nm impinges the pupil filter, which was constructed by photolithography, and placed just in the front focal plane of the focusing lens. A CCD camera (AP1E Kodak KAF-4100E) with pixel size $9\,\mu$m $\times$ $9\,\mu$m and 14 bits of dynamic range, was used to capture the intensity beam profile at various axial distances. Note that the low value of the NA allows the CCD to capture the images with good resolution. In figure 3 we display the measured and the calculated values for the axial intensity produced by the 3R filter. Note that strictly we did not measure the intensity in the axial-line points, but the intensity acquired by the central pixel of the CCD. In figure 4 we have represented, in a three-dimensional plot, the experimental three-dimensional intensity distribution provided by the 3R filter.

4. Application to single-photon fluorescence confocal microscopy

To demonstrate the utility of our proposal in single-photon fluorescence confocal microscopy, we performed numerical

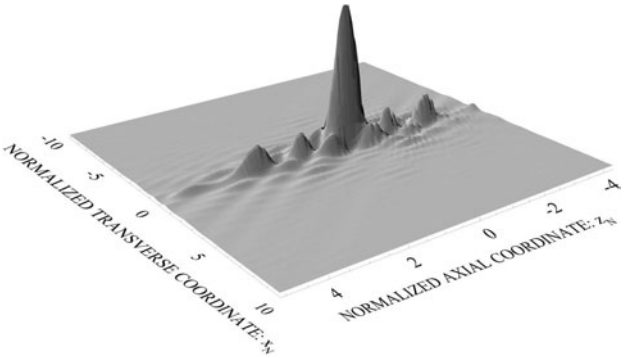

Figure 4. Experimental values of the three-dimensional intensity distribution provided by the 3R filter.

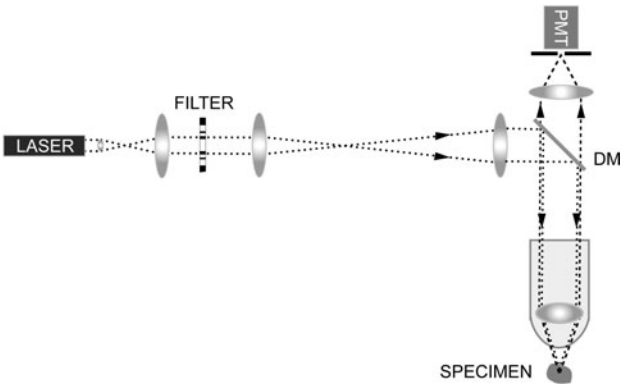

Figure 5. Schematic geometry of a single-photon fluorescence microscope. Relay lenses are used to focus the pupil filters into the back focal plane of the objective.

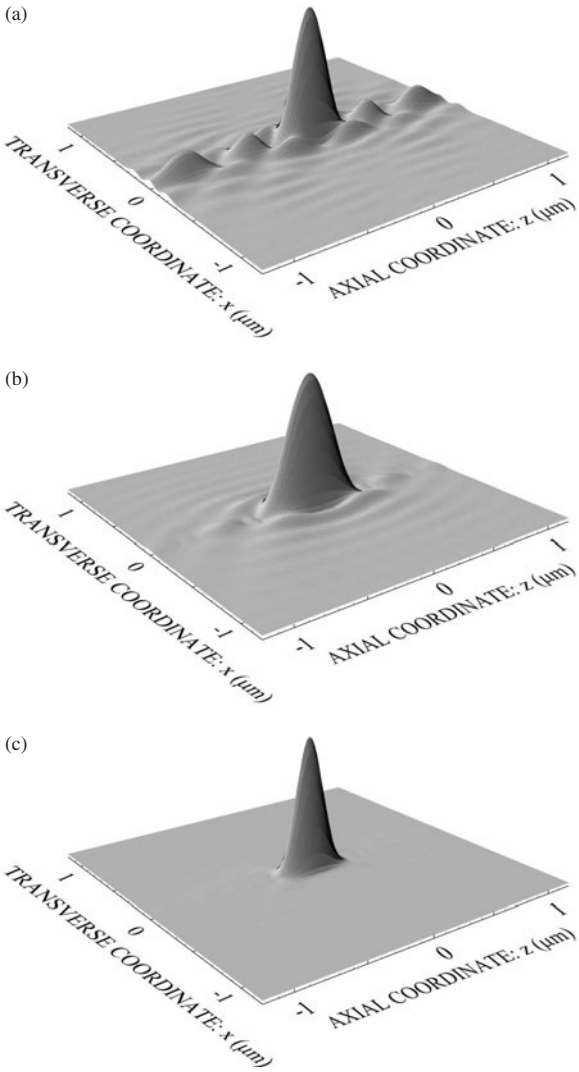

Figure 6. Plots of the three-dimensional PSF, in the meridian plane $\varphi = \pi/2$, corresponding to: (*a*) illumination arm with the 3R filter—note that this is the calculated counterpart of figure 4; (*b*) detection arm; (*c*) confocal system. The parameters for the calculation were $\lambda_{exc} = 350\,\text{nm}$, $\varepsilon = 0.8$, $n = 1.518$ and $\alpha = 67.5^{\circ}$ (NA = 1.4).

experiments by inserting the annular 3R filter in the illumination path of the confocal scheme, as shown in figure 5. In this scheme relay lenses are used to focus the filter into the front focal plane of the objective. The parameters for the calculations were $\lambda_{exc} = 350\,\text{nm}$, $\varepsilon = 0.8$, NA $= 1.4$. First we calculated the three-dimensional PSF corresponding to the illumination, the collection, and the confocal system (see figure 6). We also calculated the same PSFs but for a confocal microscope without the filter. These PSFs are depicted in figure 7. The analysis of these figures reveals an important improvement (11.3% in terms of the FWHM) of two-point axial resolution (compare figures 6(*c*) and 7(*c*)), which is obtained after a moderate increase of the illumination sidelobes. Besides, the lateral confocal PSF obtained with the 3R filter is only 0.7 % wider (in terms of the FWHM) than the PSF obtained without the filter. Therefore, it can be stated that the use of 3R filters hardly affects the transverse resolution.

When dealing with the imaging of three-dimensional objects, the three-dimensional PSF is not the best merit function to evaluate the optical sectioning capacity. A better function of merit is the axial component of the three-dimensional OTF, or equivalently its one-dimensional Fourier transform, i.e. the integrated intensity function. In practical terms the integrated intensity (also called the z-response function) can be obtained by imaging a very thin fluorescent layer which is axially scanned. Thus, in our second numerical experiment we evaluated the integrated intensity of the confocal microscope for both cases: with and without the 3R filter. These functions are plotted in figure 8. Note that, in terms of the FWHM, the use of the 3R filter sharpens the z-response by 12.3% with regard to the nonapodized microscope, resulting in a FWHM of 243 nm. Moreover, due to the special characteristics of the filters, the shoulders in the lower part of the z-response (which typically appear inherent to the use of pupil filters) are minimized.

In our third numerical experiment we considered for a value of NA which, in the absence of the 3R filter, approximately reproduces the z-response provided by the 3R filter. Both curves are plotted in figure 9. The continuous curve corresponds to the z-response of a single-photon confocal microscope that combines the 3R-filter and NA $= 1.40$, while the dashed curve corresponds to a microscope without the filter and NA $= 1.46$. It is therefore apparent that the use of our filter permits an effective increase of NA up to 1.46.

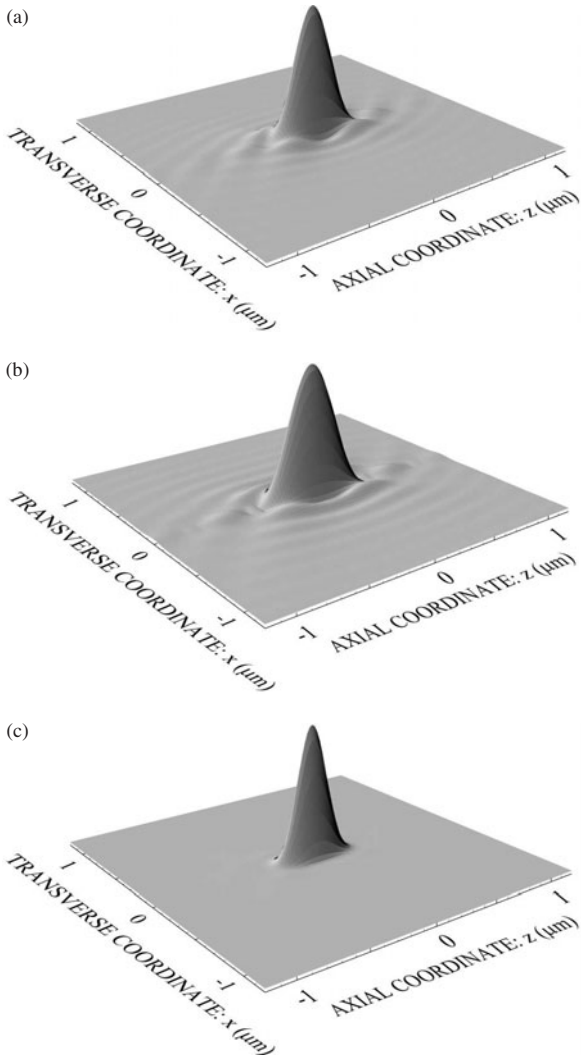

Figure 7. Same as in figure 4 but for a confocal microscope without the 3R filter.

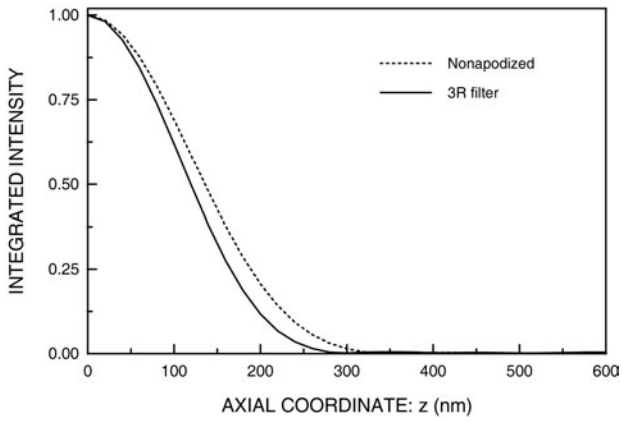

Figure 8. Theoretical z-responses of a single-photon confocal microscope. Solid curve corresponds to the apodized case in which the 3R filter is inserted in the illumination path. Dotted curve corresponds to the nonapodized case.

5. Conclusions

We have presented a new set of annular filters specifically designed to improve the axial resolution of single-photon fluorescence confocal microscopes. We numerically show that the use of these filters permits to increase the effective NA of the lenses up to 1.46. The implementation of our filter in an experimental set-up would allow to obtain an axial response with FWHM $=$ 243 nm, which would be the new lower benchmark in single-photon fluorescence microscopy.

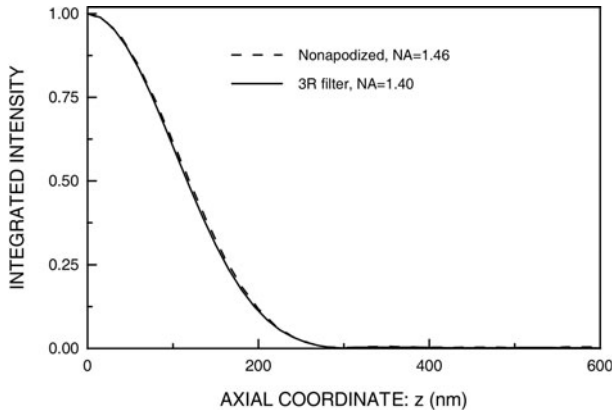

Figure 9. Theoretical z-response corresponding to a confocal microscope that combines the 3R filter and NA $=$ 1.40 (——), and to a microscope without the filter and NA $=$ 1.46 (- - - -).

Acknowledgments

This work was funded by the Plan Nacional I+D+I (Grant DPI2000-0774), Ministerio de Ciencia y Tecnología, Spain. C Ibáñez-López gratefully acknowledges financial support from the same institution.

References

[1] Wilson T (ed) 1990 *Confocal Microscopy* (London: Academic)
[2] Pawley J (ed) 1995 *Handbook of Biological Confocal Microscopy* (New York: Plenum)
[3] Stelzer E H K and Lindek S 1994 *Opt. Commun.* **111** 536–47
[4] Jonkman J E N and Stelzer E H K 2002 Resolution and contrast in confocal and two-photon microscopy *Confocal and Two-Photon Microscopy. Foundations, Applications and Advances* ed A Diaspro (New York: Wiley-Liss)
[5] Bailey B, Farkas D L, Lansing-Taylor D and Lanni F 1993 *Science* **366** 44–8
[6] Hell S and Stelzer E H K 1992 *J. Opt. Soc. Am.* A **9** 2159–66
[7] Nagorni M and Hell S 2001 *J. Opt. Soc. Am.* A **18** 36–48
[8] Nagorni M and Hell S W 2001 *J. Opt. Soc. Am.* A **18** 49–54
[9] Hegedus Z S and Sarafis V 1986 *J. Opt. Soc. Am.* A **3** 1892–6
[10] Neil M A A, Juskaitis R, Wilson T, Laczik Z J and Sarafis V 2000 *Opt. Lett.* **25** 245–7
[11] Ding Z, Wang G, Gu M, Wang Z and Fan Z 1997 *Appl. Opt.* **36** 360–3
[12] Kowalczyk M, Zapata-Rodríguez C J and Martínez-Corral M 1998 *Appl. Opt.* **37** 8206–14
[13] Sheppard C J R 1999 *Opt. Lett.* **24** 505–6
[14] Martínez-Corral M, Caballero M T, Stelzer E H K and Swoger J 2002 *Opt. Express* **10** 98–103
[15] Boyer G 2002 *J. Opt. Soc. Am.* A **19** 584–9

[16] Blanca C M and Hell S W 2002 *Opt. Express* **10** 893–8
[17] Richards B and Wolf E 1959 *Proc. R. Soc.* A **253** 358–79
[18] Martínez-Corral M, Andrés P, Ojeda-Castañeda J and Saavedra G 1995 *Opt. Commun.* **119** 491–8
[19] Martínez-Corral M, Andrés P, Zapata-Rodríguez C J and Kowalczyk M 1999 *Opt. Commun.* **165** 267–78
[20] Blanca C M, Bewersdorf J and Hell S W 2001 *Appl. Phys. Lett.* **79** 2321–3
[21] Boyer G R 1983 *Opt. Acta* **30** 807–16